

A fast multiparameter MRI approach for acute stroke assessment on a 3T clinical scanner: preliminary results in a non-human primate model with transient ischemic occlusion

Xiaodong Zhang¹, Frank Tong², Chun-Xia Li¹, Yumei Yan¹, Govind Nair^{1,3,4}, Tsukasa Nagaoka^{1,5}, Yoji Tanaka^{1,6}, Stuart Zola^{1,7}, Leonard Howell^{1,7}

¹Yerkes National Primate Research Center, Emory University, Atlanta, GA 30329, USA; ²Department of Radiology, School of Medicine, Emory University, Atlanta, GA 30322, USA; ³the Wallace H. Coulter Department of Biomedical Engineering, Emory University and Georgia Institute of Technology, Atlanta, GA 30322, USA; ⁴National Institute of Neurological Disorders and Stroke, National Institutes of Health, Bethesda, MD 20892, USA; ⁵Sony Corporation, Tokyo, Japan; ⁶Department of Neurosurgery, Tokyo Medical and Dental University, Tokyo, Japan; ⁷Department of Psychiatry and Behavioral Sciences, School of Medicine, Emory University, Atlanta, GA 30322, USA

Correspondence to: Xiaodong Zhang, PhD. Yerkes Imaging Center, Yerkes National Primate Research Center, Emory University, 954 Gatewood Rd NE, Atlanta, GA 30329, USA. Email: xzhang8@emory.edu.

Abstract: Many MRI parameters have been explored and demonstrated the capability or potential to evaluate acute stroke injury, providing anatomical, microstructural, functional, or neurochemical information for diagnostic purposes and therapeutic development. However, the application of multiparameter MRI approach is hindered in clinic due to the very limited time window after stroke insult. Parallel imaging technique can accelerate MRI data acquisition dramatically and has been incorporated in modern clinical scanners and increasingly applied for various diagnostic purposes. In the present study, a fast multiparameter MRI approach including structural T1-weighted imaging (T1W), T2-weighted imaging (T2W), diffusion tensor imaging (DTI), T2-mapping, proton magnetic resonance spectroscopy, cerebral blood flow (CBF), and magnetization transfer (MT) imaging, was implemented and optimized for assessing acute stroke injury on a 3T clinical scanner. A macaque model of transient ischemic stroke induced by a minimal interventional approach was utilized for evaluating the multiparameter MRI approach. The preliminary results indicate the surgical procedure successfully induced ischemic occlusion in the cortex and/or subcortex in adult macaque monkeys (n=4). Application of parallel imaging technique substantially reduced the scanning duration of most MRI data acquisitions, allowing for fast and repeated evaluation of acute stroke injury. Hence, the use of the multiparameter MRI approach with up to five quantitative measures can provide significant advantages in preclinical or clinical studies of stroke disease.

Keywords: Stroke; monkey model; GRAPPA; diffusion tensor imaging (DTI); arterial spin tagging; continuous arterial spin labeling (CASL), cerebral blood flow (CBF); *in vivo* spectroscopy; magnetization transfer (MT); multimodality MRI; parallel imaging

Submitted Feb 03, 2014. Accepted for publication Apr 21, 2014.

doi: 10.3978/j.issn.2223-4292.2014.04.06

View this article at: <http://www.amepc.org/qims/article/view/3731/4652>

Introduction

MRI has been increasingly used to characterize stroke injury in infarct age, volume and territory, clotted vascular structure, degree of hypoperfusion, cerebral metabolite, penumbra evolution, and viability of tissue at risk after stroke onset

(1-5). As each MRI parameter can be associated with one or multiple specific tissue structural or physiological properties, the combined usage and analysis of these complementary MRI parameters, or multiparameter MRI approach, can provide integrated and systematic information about the

ischemic cascade after stroke insult. However, due to the intrinsic limitation of MRI techniques [each k-space line is usually acquired after every repetition time (TR)] and physiological limitations [rapidly switched gradients result in neuromuscular stimulation and excessive radio frequency (RF) pulses cause RF power over-exposure and tissue heating], one MRI measurement can take from minutes to hours to obtain optimal images. As speed is a critical consideration in acute stroke imaging, multiparameter MRI in clinic is usually conducted with only 2-3 MRI modalities [mostly diffusion-weighted imaging (DWI), perfusion MRI, and T2-weighted imaging (T2W)], limiting its effectiveness and application in acute stroke examination. The advent of parallel imaging with multichannel RF coils lead to a dramatic acceleration of imaging speed in conventional MRI scans, resulting in revolutionary advances in MRI techniques and increasing applications in the clinic and preclinical studies (6-8). Therefore, parallel imaging technique can provide an effective approach to facilitate multiparameter MRI studies in stroke disease.

In comparison with popular rodent models of stroke, non-human primates (NHPs) are most closely related to human beings in anatomy, physiology, social complexity and cognitive capabilities. Many NHP models of stroke have been explored successfully (9-15), allowing for stroke disease to be evaluated under controlled conditions and examined with various non-invasive methods including imaging, behavior and neurological examination. Therefore, the NHP models together with multiparameter MRI approach can provide an ideal platform for studying the pathophysiological mechanism of stroke disease and therapeutic development. In the present study, a fast multiparameter MRI approach was implemented using parallel imaging technique and optimized for examining the acute stroke injury in a macaque model with transient ischemic occlusion.

Methods and materials

Subjects

Adult rhesus monkeys (n=4, female, 6.3-11.3 kg, 9-15 years old) were utilized in the present study (*Table 1*). The subjects were initially anesthetized with ketamine (5-10 mg/kg, IM), then orally intubated. During surgery and MRI scanning, animals were anesthetized with 1-1.5% isoflurane mixed with 100% O₂ while spontaneously-breathing. Body temperature was maintained at 37.5 °C by a feedback-regulated circulating warm-water blanket. In order to restrain the subjects for

surgery and MRI scanning, anesthetized subjects were further immobilized with a custom-made head holder and placed in the “supine” position which is generally used in clinical MRI for patients. Et-CO₂, inhaled CO₂, O₂ saturation, blood pressure, mean arterial pressure (MAP), heart rate, respiration rate, and body temperature were monitored continuously and maintained in normal ranges (16). The procedures were approved by the Institutional Animal Care and Use Committee (IACUC) of Emory University in accordance with the NIH Guide for Care and Use of Laboratory Animals.

Transient cerebral ischemia was induced by middle cerebral artery (MCA) occlusion with a minimal invasive interventional approach (13). Briefly, a microcatheter was inserted into the femoral artery under fluoroscopic guidance and the distal M2 section of MCA was occluded with a microcatheter tip (n=2) or microcoil (n=2) for 3 hours. The MCA occlusion of each subject was confirmed by digital subtraction angiography (Siremobil Compact L fluoroscopic system, Siemens Medical Solutions USA, Inc, Malvern, PA, USA). The reperfusion (microcatheter or microcoil removal) occurred under fluoroscopy (before the animals were moved to MRI).

MRI evaluation

MRI was performed using a Siemens 3T Trio clinical scanner (Siemens Medical Solutions USA, Inc, Malvern, PA, USA) equipped with an 8-channel phased-array knee coil (Invivo Inc, FL, USA). Imaging modalities included: MR angiography (MRA) by time of flight (TOF) sequence, T1-weighted imaging (T1W) by a 3D magnetization-prepared rapid acquisition gradient echo (MPRAGE) sequence, T2W by fast spin-echo sequence, magnetization transfer (MT) imaging or magnetization transfer contrast (MTC) MRI by a custom-designed echo-planar imaging (EPI) sequence, diffusion tensor imaging (DTI) by single-shot EPI, and quantitative cerebral blood flow (CBF) using continuous arterial spin labeling (CASL) (17,18). Proton MR Spectroscopy was conducted using the chemical shift imaging (CSI) or MR spectroscopic imaging (MRSI) sequence with weighted phase-encoding acquisition, outer-volume tissue suppression and CHESS water suppression (19,20). The generalized autocalibrating partially parallel acquisitions (GRAPPA) reconstruction strategy was utilized for parallel imaging acceleration. The MRI acquisition parameters of each measure were illustrated in *Table 2*. In addition, each ASL scan had 40 pairs of control and label images and each MTC scan had 8 measurements for signal average.

Table 1 Demographic data for animal age, body weight, stroke occluder, and infarct volume after 3-hour transient MCA occlusion.

Animal ID	RTM5	RWV4	RLB6	RYL7
Age (years)	14.7	11.8	12.5	9.5
Body weight (kg)	9.2	11.3	7.7	6.3
Occluder	Microcatheter tip	Microcatheter tip	Microcoil	Microcoil
Infarct volume (half hours after reperfusion)	0.32	2.10	0.20	0.34
Infarct volume (two and half hours after reperfusion)	0.33	2.80	0.20	0.91

MCA, middle cerebral artery.

Table 2 MRI experimental parameters for MRA, T1W, T2W, DTI, ASL-CBF, MTC, T2, and proton MRS of stroke monkeys on a clinical 3T scanner

	MRA	T1W	T2W	DTI	ASL-CBF	MTC	T2	MRS
TR (ms)	39	2,400	6,300	5,000	3,830	2,220	5,780	1,700
TE (ms)	7.33	3.73	125	87	21	20	9.1/64/82/146	30
FOV (mm)	112×112	116×116	96×96	96×96	96×96	96×96	96×96	64×64
Data matrix	448×448	192×192	192×192	64×64	64×64	64×64	128×128	16×16
Number of averages	2	2	2	4	4	1	1	4
Flip angle (degree)	15	8	90	90	90	90	90	70
Bandwidth (Hz)	147	130	110	1,346	1,698	1,474	399	1,200
Voxel size (mm ³)	0.25×0.25×1	0.6×0.6×0.6	0.5×0.5×1.5	1.5×1.5×1.5	1.5×1.5×1.5	1.5×1.5×1.5	0.75×0.75×1.5	4×4×10
Scan duration (minutes)	7:44	6:40	3:09	12:02	20:56	3:04	3:35	8:10

MRA, MR angiography; T1W, T1-weighted imaging; T2W, T2-weighted imaging; DTI, diffusion tensor imaging; ASL, arterial spin labeling; CBF, cerebral blood flow; MTC, magnetization transfer contrast; MRS, MR spectroscopy.

Immediately after the reperfusion, the monkeys were moved into the MRI scanner and examined with MRA, T2W, T1W for vascular and anatomical imaging, and T2, CBF, DTI, MTC, MRS measurements for quantitative evaluation of the stroke injury. The time between the removal of occluder and acquisition of the first MRI scan was 30 minutes or less. DTI images were collected at 0.5, 1.5, 2.5 hours post reperfusion. CBF data were collected at 0.75 and 2.75 hours post reperfusion. Structural T1W images were collected before and after intravenous Gadolinium contrast agent injection (0.02 mg/kg, IV; Omniscan, GE Healthcare, USA). All the MRI measurements were accomplished by using the single setting with the phased-array volume coil.

In addition, for comparison purpose, the MRI protocols were tested and compared with a comparable quadrature volume coil (Siemens extremity knee coil, Siemens Medical Solutions USA, Inc, Malvern, PA, USA) on a normal healthy adult rhesus monkey.

MRI data processing

The MRA, T2W, T1W images were processed and displayed with the Syngo medical imaging software in the Siemens 3T scanner console. MRS data was processed with the Siemens spectroscopy package in the console. DTI images were processed with the DTIstudio software (21). T2, MTC, CBF maps, stroke infarct volume were calculated with the home-built Matlab scripts (MathWorks Inc, MA, USA). The infarct volume of each subject was estimated from the mean diffusivity (MD) maps (22).

Histology

Animals were sacrificed immediately by pentobarbital overdose for brain harvesting without recovery from isoflurane anesthesia after the MRI examination. Intracardial perfusion was conducted with saline followed by 10% buffered formalin. Hematoxylin and eosin (H&E)

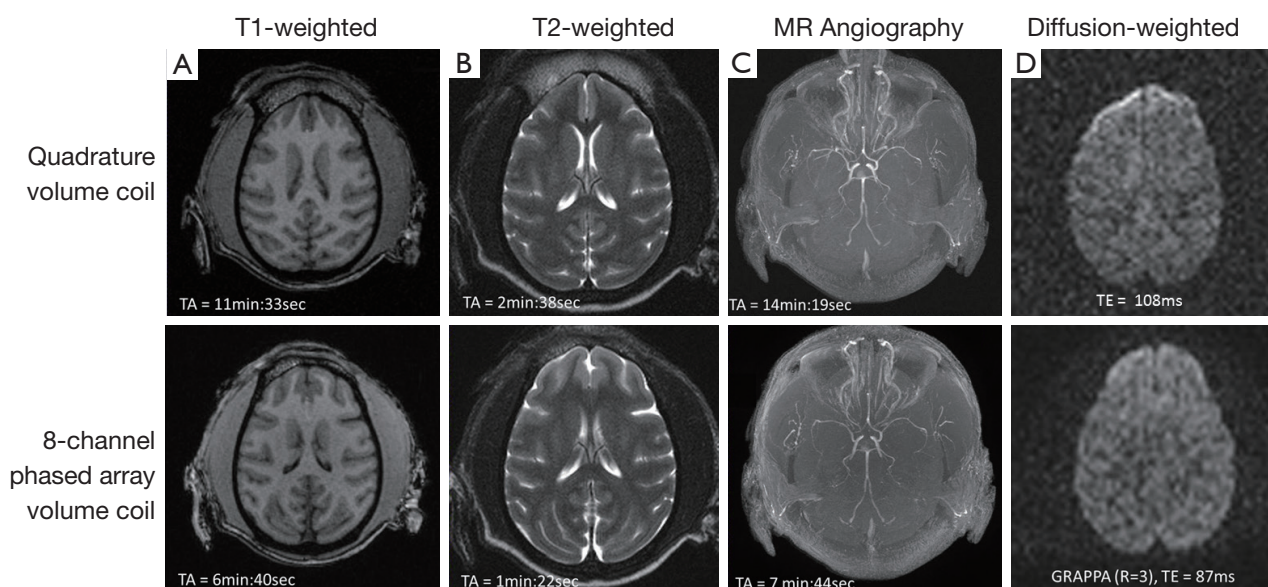


Figure 1 Comparison of various MRI images. (A) T1-weighted; (B) T2-weighted; (C) MR angiography; (D) diffusion-weighted images of an adult monkey brain acquired with and without parallel imaging (GRAPPA). Top, using quadrature volume coil; bottom, using 8-channel phased-array volume coil; TA, acquisition time.

staining was performed for validating the stroke lesion.

Results

MRI data acquisition optimization

The monkey brain imaging protocols including T1W, T2W, MRA, and DTI were evaluated with the 8-channel phased-array volume coil and Siemens extremity quadrature volume coil. As shown in *Figure 1*, the scanning duration for T1W, T2W, MRA with GRAPPA were reduced by almost 50% with the image quality comparable to that acquired with the regular quadrature coil setting without parallel imaging. Meanwhile, the DWI images derived from DTI with parallel imaging acquisition show evident distortion reduction in the frontal lobe in comparison with that acquired without parallel imaging. In addition, regular EPI images acquired with GRAPPA (R =2) have similar TE (20 vs. 21 ms) as those with the partial Fourier acquisition strategy (23,24). As the EPI images acquired with partial-Fourier showed slightly higher signal to noise ratio (SNR) than that with GRAPPA, the partial-Fourier (R =6/8) acquisition was used in the CASL scans. No GRAPPA was applied in the CSI scan due to the tradeoff of SNR decrease in parallel imaging technique.

The optimization results of regular and diffusion weighted EPI sequences are shown in *Figure 2*. Compared

with the images acquired with standard sequence and partial-Fourier acquisition strategy, the GRAPPA acceleration factor R =2 offers optimal image quality for general EPI images and R =3 for diffusion weighted images. In particular, the image distortion artifact in the frontal lobe was reduced significantly.

The scanning duration for quantitative MRI measures including T2 map, ASL-CBF, DTI indices, MTC, MRS were about 3, 20, 12, 3, 8 minutes, respectively. Therefore, all the quantitative measurements can be accomplished within one hour, allowing the stroke evolution to be assessed hourly with the proposed multiparameter MRI approach after stroke onset.

Stroke injury evaluation with MRI

After the stroke animals were transferred into the scanner, DTI and MRA were conducted firstly to evaluate the vessel occlusion and stroke lesion, and then followed with ASL-CBF, MTC, T2W, T2 maps and CSI. Lastly, T1W images were collected before and after Gadolinium agent injection. DTI and CBF scans were repeated three and two times respectively. Occluded MCA in a stroke subject is shown in the MRA image (*Figure 3*). The corresponding stroke lesion is exhibited explicitly in the T2W and DWI images, T2, MTC and MD maps (with arrows). Based upon the

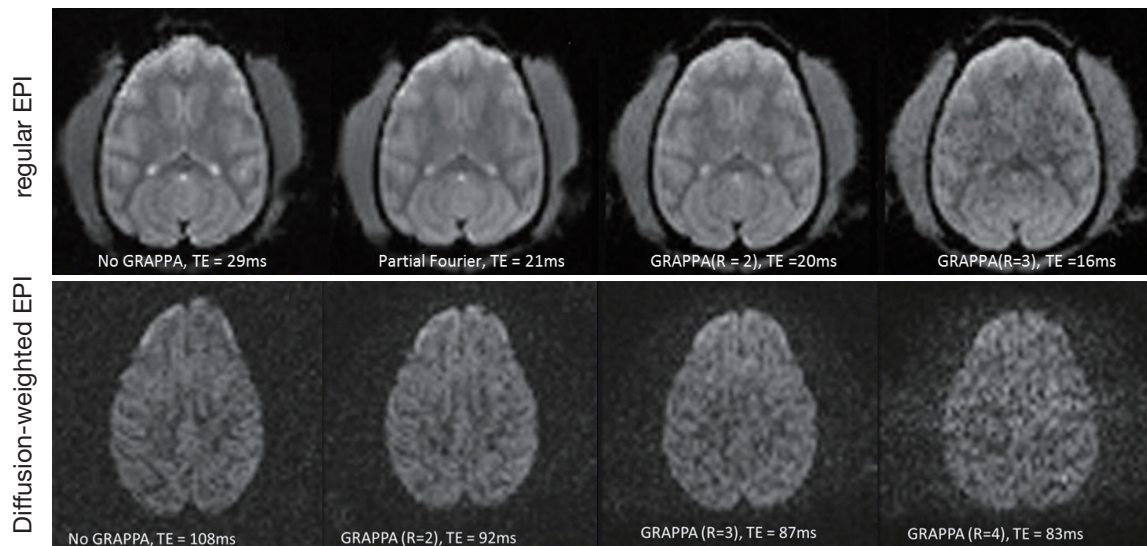


Figure 2 Comparison of regular EPI and DWI images of an adult monkey brain. Top, regular EPI images acquired with no GRAPPA, partial-Fourier, GRAPPA (R=2) and GRAPPA (R=3); bottom, DWI images acquired with no GRAPPA, GRAPPA (R=2), GRAPPA (R=3), and GRAPPA (R=4), b value =1,000 s/mm². EPI, echo-planar imaging; GRAPPA, generalized autocalibrating partially parallel acquisitions.

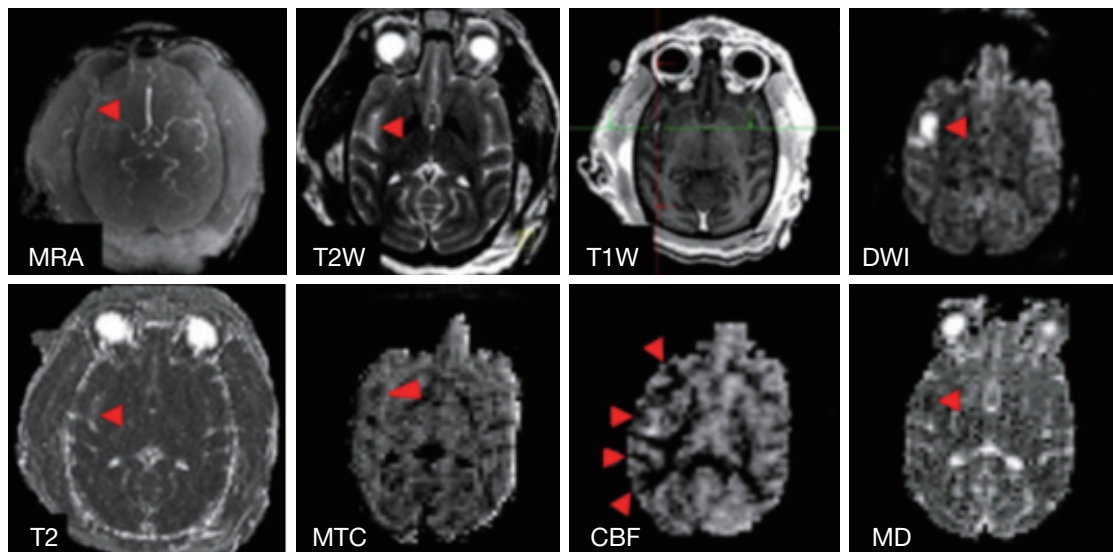


Figure 3 Illustration of stroke lesion. Top, MR Angiography, T2W, T1W, and DWI images of an adult stroke monkey (RLB6) post reperfusion; bottom: quantitative MRI measures (T2, MTC, CBF, and MD maps) of the same monkey. The monkey (RLB6) was induced with 3-hour transient MCA occlusion. Arrows: stroke-injured regions. MRA, MR angiography; T2W, T2-weighted imaging; T1W, T1-weighted imaging; MTC, magnetization transfer contrast; CBF, cerebral blood flow; MD, mean diffusivity; MCA, middle cerebral artery.

T1W images post gadolinium injection, no hemorrhage was observed in any subject. Also, stroke-induced hypoperfused regions are observed in the CBF map (pointed with arrows).

The progressive CBF changes in the whole brain of a stroke subject after 3-hour transient MCA occlusion are

illustrated (*Figure 4*), revealing slight CBF changes from the 0.75 to 2.75 hours post reperfusion. The stroke infarct volumes are tabulated in *Table 1*. The results demonstrate that the infarct volume increased after reperfusion in two subjects (RWV4 and RYL7). In comparison, the infarct

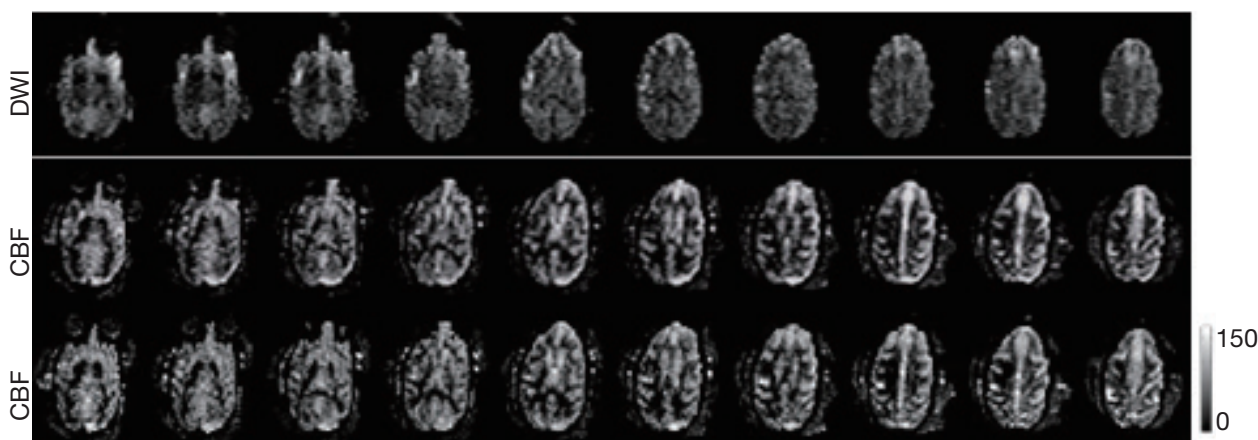


Figure 4 Illustration of stroke lesion in the monkey RLB6 with 3-hour transient MCA occlusion. Top, DWI images half hours post reperfusion; Middle, CBF maps 0.75 hours post reperfusion; bottom, CBF maps 2.75 hours post reperfusion. Ten slices were selected for demonstration. CBF unit, mL/100 g/min. CBF, cerebral blood flow; MCA, middle cerebral artery.

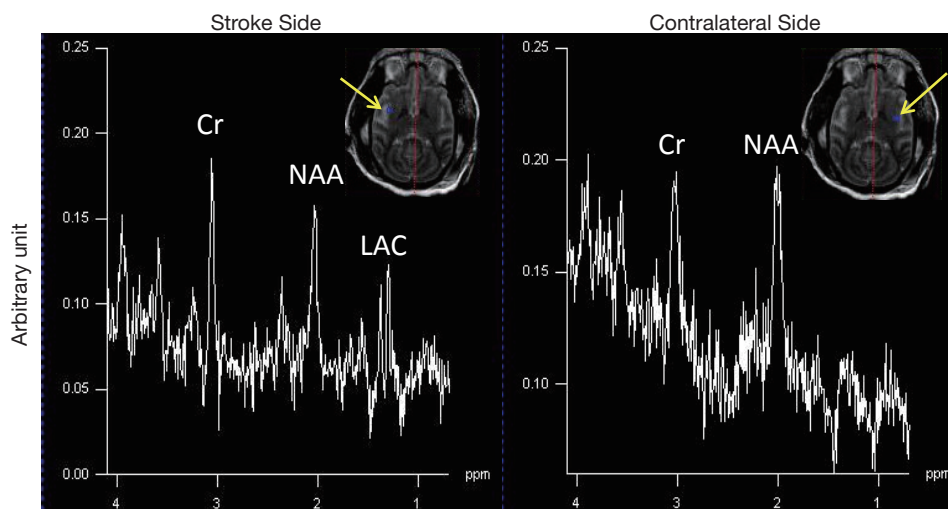


Figure 5 *In vivo* proton spectra on the lesion side (left) and contralateral side (right) of a stroke monkey (RLB6), acquired with two-dimensional chemical shift imaging (2D CSI), two and a quarter hours post reperfusion. Cr, creatine; NAA, N-acetylaspartate; LAC, lactate. Arrow: voxel location.

volumes of the subjects RTM5 and RLB6 remained almost unchanged after reperfusion. Also, as shown in *Figure 5*, reduced NAA and increased lactate were observed after reperfusion. The stroke lesion of the subject RWV4 was further validated using H&E staining (*Figure 6*).

Discussion

The application of parallel imaging technique dramatically reduced the scanning duration in MRA, T1W, T2W, and improved the imaging quality of DTI images of macaque brain. Also, all the measurements were accomplished with

a single setting, enabling the MRA, T1W, and T2W scans together with multiple quantitative imaging modalities including T2, DTI indices (FA and MD), CBF, MTC, and MRS to be conducted within one hour for temporal evaluation of acute stroke injury in a NHP model of ischemic stroke.

Imaging acceleration in MRA, T1W, T2W scans and image quality improvement in DTI images with GRAPPA

High-resolution T1-weighted images acquired with the MPRAGE sequence are generally used for structural

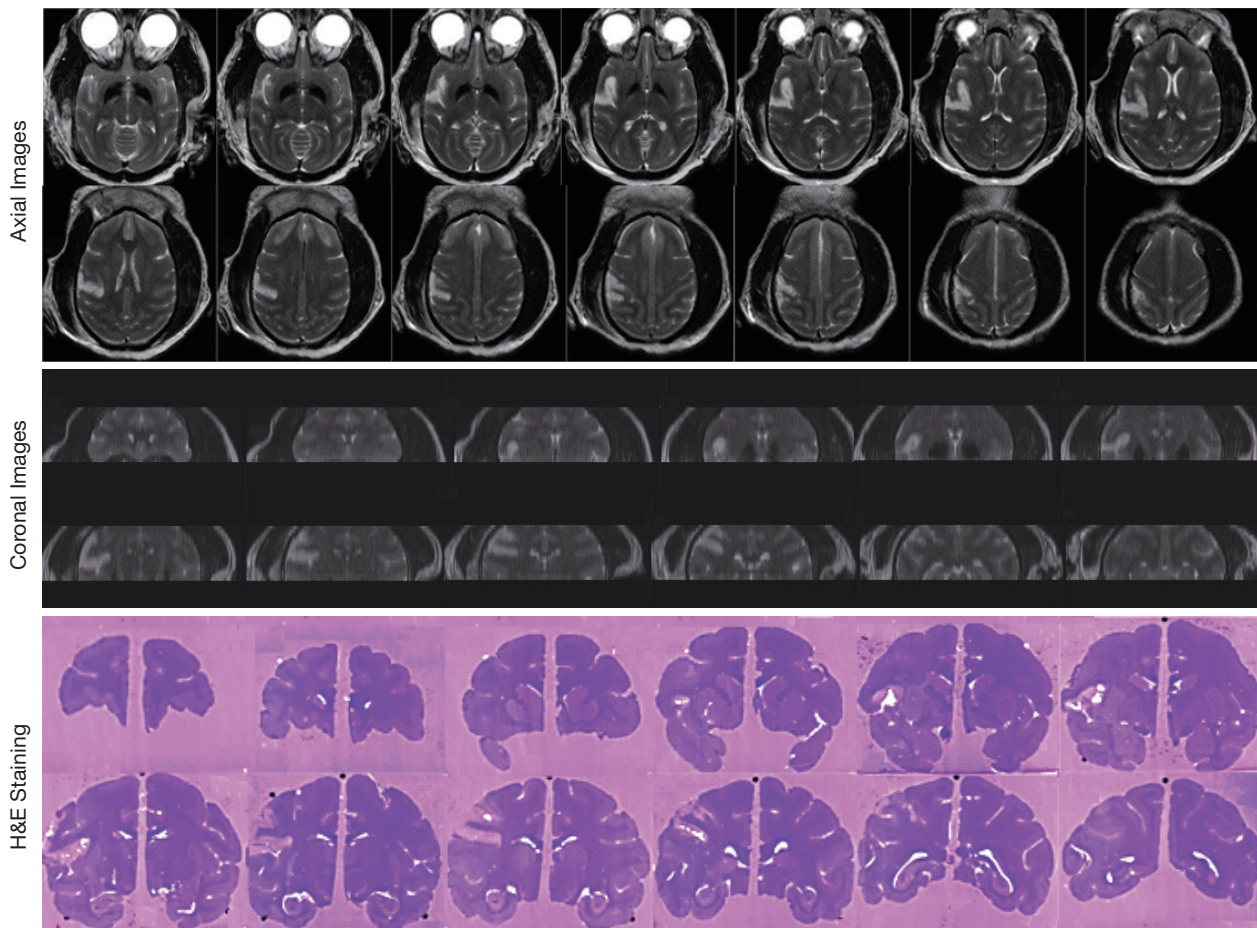


Figure 6 Illustration of stroke lesion. Top, axial T2W images of a stroke monkey (RWV4) 2.5 hours post reperfusion; Middle, reconstructed coronal T2W images of the same stroke monkey; bottom: H&E staining of the same stroke monkey brain.

identification, segmentation or brain volumetric analysis. A prior clinical study has demonstrated that the application of parallel imaging with GRAPPA dramatically reduced the MPRAGE acquisition time (TA) without introducing detrimental effect to brain tissue segmentation and volumetric measurement (25). In the present study, no obvious difference in T1W images was seen visually between the scans acquired with the regular quadrature and phased-array coils (*Figure 1*).

As seen in *Figure 1*, application of parallel imaging technique and the 8-channel phased-array coil results in a dramatic (~50%) reduction in T1W, T2W, and MRA scan durations while keeping sufficient quality for illustrating the anatomical structures of monkey brain. As T2 map is derived from serial T2W images acquired with different TEs, the corresponding scanning duration is reduced considerable as well. Accordingly, parallel imaging

technique allows more imaging modalities to be conducted within a limited time window.

DTI is a non-invasive MRI technique to detect the water diffusivity of brain tissue *in vivo* and has been used widely in stroke studies (26-30). As DTI is usually performed by using a single-shot spin-echo EPI sequence with long TE and strong gradient pulses, DTI images are complicated with susceptibility artifacts and eddy-current induced effects which become severe in the high and ultrahigh magnetic field scanners. In comparison with human brain, macaque brain is much smaller (1,200-1,300 vs. ~100 cc). Therefore, much higher spatial resolution is required to achieve acceptable image quality. Clinical MRI scanners have large magnet bore which facilitates animal handling and experimental setting significantly. However, these scanners are usually equipped with lower gradient strength (4 G/cm) and limited B0 shimming system compared to regular

animal scanners (40 G/cm or more). Therefore, DTI images of a macaque brain can be complicated with severe image distortion and susceptibility artifacts due to increased spatial resolution required for a small brain. The present optimization results exhibit the relationship between GRAPPA acceleration factor and DTI image quality, and demonstrate that optimal DTI images can be obtained by using parallel imaging technique with a clinical setting. Thus, the further integrated data analysis can be facilitated with the improved image quality.

Anatomical and quantitative MRI measurements

Stroke results in a pathophysiological cascade of metabolite, microstructural, molecular and cellular changes. Many MRI parameters have been explored and demonstrated the capability and potential to assess stroke injury. Briefly, (I) DWI is known to be the most sensitive MRI modality to detect a cerebral infarct in minutes after stroke insult (31). Also, apparent diffusion coefficient (ADC) (derived from DWI images) decreases over time during acute stroke and then returns to the pseudonormal value. The combined DWI images and ADC maps may be used to estimate the infarct territory and age (32). In contrast, DTI can offer much more complimentary information including the tissue diffusivity (radial and axial diffusivity, MD or ADC) and fractional anisotropy (FA). Especially it allows for detecting the white matter microstructural disruption in stroke injury or brain remodeling in chronic stage (26,28,29), and may be more sensitive than DWI to white matter ischemia (33); (II) hyperintense in T2W images reveals the vascular brain edema in acute ischemic stroke. T2-value is dependent on brain tissue water content and changes over time after stroke onset (34) and is a quantitative measure to detect water uptake in ischemic tissue (1,35); (III) artery occlusion results in immediate CBF reduction in the corresponding territory of the occluded vessel and the absolute CBF values indicate the cell viability after stroke insult. Most importantly, the diffusion-perfusion mismatch approximates the ischemic penumbra and has been used as a surrogate marker of the tissue at risk (4,22); (IV) magnetization transfer imaging can be used to detect macromolecular disruption. Previous results have showed the potential to detect edema and loss of cellular structure during the progression of ischemic stroke in patients and rodents (36,37); (V) the blood-brain-barrier (BBB) permeability disruption is usually seen in stroke brains and may cause hemorrhage complication. T1W images post Gadolinium

injection can reveal the possible hemorrhage and abnormal volumetric changes due to swelling in acute stroke as well.

As illustrated in the MRA image (*Figure 3*), the M2 section of MCA was still occluded after reperfusion probably due to secondary clot formation or vasospasm after catheter intervention. The cortical infarct is seen on T2W and DWI images. In addition, the abnormality is observed in quantitative measures including T2, MTC, MD (marked with arrows), consistent with the DWI finding (*Figure 3*). CBF reduction is seen in the cortical and subcortical regions (labeled with arrows). Benign oligemia is also observed in the subcortical regions most likely due to the surgical procedure as mentioned above. Progressive CBF measurements of the whole stroke monkey brain exhibit slight regional changes in brain hemodynamics after reperfusion (*Figure 4*). The present results suggest that a longitudinal survival study in the future should provide more comprehensive and quantitative assessment of stroke injury.

In addition, it is known that cerebral ischemia results in intracellular metabolism alteration after stroke onset. Increased lactate and reduced NAA reveal the abnormal status of cellular metabolism after stroke injury (5,38-40). In particular, proton MRS can reveal the abnormal neuronal death in the region adjacent to the stroke infarct while it appears normal in the T1W and T2W images (41). The metabolite alternation in a stroke monkey is illustrated after transient stroke attack (*Figure 5*). Obviously, the MCA occlusion caused the NAA reduction and lactate elevation in the injured brain region, in agreement with previous findings in stroke patients and animals (38,41-44).

Stroke infarct evaluation during acute ischemic stroke

In the present study, micro-catheter tip and endovascular microcoil (usually used for brain aneurysm treatment) were used as occluders to induce 3-hour MCA occlusion in adult macaque monkeys (n=2 for each occluder). As seen in *Table 1*, lesion sizes varied across the four animals and the microcoil may induce more consistent infarction than a microcatheter tip. However, the variation of infarction volume might be mainly caused by the MCA collateralization in each monkey (45). Also, the infarct volumes in two animals (RTM5, RLB6) remained almost unchanged in the following 3 hours after reperfusion probably due to the developed collateral circulation in these two animals.

Multiparameter MRI is generally incorporated in the high-field or ultra-high, small-bore research scanner which is equipped with enhanced gradient system and abundant

pulse sequences for different imaging purposes in preclinical studies. In contrast, these hardware and software resources are not readily available in most clinical scanners with much lower gradient strength and conventional MRI protocols for general clinical diagnostic purposes. Any non-standard imaging protocols such as ASL perfusion or MT imaging, or most novel MRI pulse sequences, will require specific development and optimization. As demonstrated in the present study, a fast multiparameter MRI approach for imaging stroke macaques was implemented by combining conventional clinical protocols and custom-developed pulse sequences in a high-field clinical setting. Especially, the multiple quantitative MRI parameters (T2, CBF, DTI indices, MTC, MRS) can be obtained within one hour for a macaque model of stroke, allowing integrated information to be collected with high temporal resolution during hyperacute stroke. Certainly, other stroke-related MRI measures such as ATP (46), T1- ρ (47,48), K_{trans} (49) *et al.*, can be added for different research purposes. Meanwhile, the current ASL-based perfusion measurement can be improved with pseudo-continuous ASL (pCASL) (50,51) or 3D gradient and spin echo (GRASE) (52) ASL technique. Certainly, a two- or three-coil setting ASL technique will offer optimal CBF measurement for macaques (16,53). Also, the image results shown in this report are mainly used for quick evaluation of stroke lesion. More deliberate MRI data processing can be conducted with the dedicated software packages such as FSL (www.fmrib.ox.ac.uk/fsl) for functional or structural image analysis and LCMoDe (www.s-provencher.com) for *in vivo* MR spectrum analysis.

In addition, due to the ethics and high cost of NHP species, the usage of NHPs (or other large animals) is much more limited than that of rodents. The multiparameter approach allows for maximal data collection in each animal to minimize the animal numbers or sample size in each study. Therefore, the use of multiple MRI parameter approach can be a powerful and effective means for studying the structural and physiological alteration and therapeutic development following stroke or other diseases in large animals.

In conclusion, the application of parallel imaging technique substantially reduces TA of most time-consuming MRI measurements and allows fast and/or repeated examination of acute stroke injury with a multiparameter MRI approach. The established protocols are validated with a macaque model of stroke in a clinical setting and can be used for assessing the temporal evolution of stroke injury in NHP stroke models or likely in stroke patients. In fact, the translation of this approach to stroke patients will even

benefit from the larger volume of the human brain.

Acknowledgements

The authors thank Sudeep Patel for MRI data collection, Ruth Connelly, Wendy Williamson Coyne, Juliet Brown, Jean Ksiazek, Dr Fawn Connor-Stroud (DVM) for animal care in MRI and surgery; Dr Anapatricia Garcia for necropsy; Drs Manuel Yepes, Byron Ford, Shan Ping Yu, Ling Wei for their thoughtful suggestions. This project was supported in part by NCRR and currently by the Office of Research Infrastructure Programs (OD P51OD011132, P51RR000165 and OD P51OD011132), and by the National Center for Advancing Translational Sciences of the National Institutes of Health under Award Number UL1TR000454.

Disclosure: The authors declare no conflict of interest.

References

- Jacobs MA, Mitsias P, Soltanian-Zadeh H, et al. Multiparametric MRI tissue characterization in clinical stroke with correlation to clinical outcome: part 2. *Stroke* 2001;32:950-7.
- Nagaraja TN, Knight RA, Ewing JR, et al. Multiparametric magnetic resonance imaging and repeated measurements of blood-brain barrier permeability to contrast agents. *Methods Mol Biol* 2011;686:193-212.
- Alexandrov AV, Rubiera M. Use of neuroimaging in acute stroke trials. *Expert Rev Neurother* 2009;9:885-95.
- Ebinger M, De Silva DA, Christensen S, et al. Imaging the penumbra - strategies to detect tissue at risk after ischemic stroke. *J Clin Neurosci* 2009;16:178-87.
- Saunders DE. MR spectroscopy in stroke. *Br Med Bull* 2000;56:334-45.
- Sodickson DK, McKenzie CA, Ohliger MA, et al. Recent advances in image reconstruction, coil sensitivity calibration, and coil array design for SMASH and generalized parallel MRI. *MAGMA* 2002;13:158-63.
- Deshmane A, Gulani V, Griswold MA, et al. Parallel MR imaging. *J Magn Reson Imaging* 2012;36:55-72.
- Larkman DJ, Nunes RG. Parallel magnetic resonance imaging. *Phys Med Biol* 2007;52:R15-55.
- Watanabe O, West CR, Bremer A. Experimental regional cerebral ischemia in the middle cerebral artery territory in primates. Part 2: Effects on brain water and electrolytes in the early phase of MCA stroke. *Stroke* 1977;8:71-6.
- Marshall JW, Ridley RM, Baker HF, et al. Serial MRI,

- functional recovery, and long-term infarct maturation in a non-human primate model of stroke. *Brain Res Bull* 2003;61:577-85.
11. Bihel E, Roussel S, Toutain J, et al. Diffusion tensor MRI reveals chronic alterations in white matter despite the absence of a visible ischemic lesion on conventional MRI: a nonhuman primate study. *Stroke* 2011;42:1412-9.
 12. West GA, Golshani KJ, Doyle KP, et al. A new model of cortical stroke in the rhesus macaque. *J Cereb Blood Flow Metab* 2009;29:1175-86.
 13. de Crespigny AJ, D'Arceuil HE, Maynard KI, et al. Acute studies of a new primate model of reversible middle cerebral artery occlusion. *J Stroke Cerebrovasc Dis* 2005;14:80-7.
 14. Cook DJ, Tymianski M. Nonhuman Primate Models of Stroke for Translational Neuroprotection Research. *Neurotherapeutics* 2012;9:371-9.
 15. Cook DJ, Teves L, Tymianski M. Treatment of stroke with a PSD-95 inhibitor in the gyrencephalic primate brain. *Nature* 2012;483:213-7.
 16. Li CX, Patel S, Auerbach EJ, et al. Dose-dependent effect of isoflurane on regional cerebral blood flow in anesthetized macaque monkeys. *Neurosci Lett* 2013;541:58-62.
 17. Li C, Zhang X, Komery A, et al. Longitudinal diffusion tensor imaging and perfusion MRI investigation in a macaque model of neuro-AIDS: a preliminary study. *Neuroimage* 2011;58:286-92.
 18. Wang J, Zhang Y, Wolf RL, et al. Amplitude-modulated continuous arterial spin-labeling 3.0-T perfusion MR imaging with a single coil: feasibility study. *Radiology* 2005;235:218-28.
 19. Maudsley AA, Matson GB, Hugg JW, et al. Reduced phase encoding in spectroscopic imaging. *Magn Reson Med* 1994;31:645-51.
 20. Zhang X, Heberlein K, Sarkar S, et al. A multiscale approach for analyzing in vivo spectroscopic imaging data. *Magn Reson Med* 2000;43:331-4.
 21. Jiang H, van Zijl PC, Kim J, et al. DtiStudio: resource program for diffusion tensor computation and fiber bundle tracking. *Comput Methods Programs Biomed* 2006;81:106-16.
 22. Shen Q, Meng X, Fisher M, et al. Pixel-by-pixel spatiotemporal progression of focal ischemia derived using quantitative perfusion and diffusion imaging. *J Cereb Blood Flow Metab* 2003;23:1479-88.
 23. McGibney G, Smith MR, Nichols ST, et al. Quantitative evaluation of several partial Fourier reconstruction algorithms used in MRI. *Magn Reson Med* 1993;30:51-9.
 24. Zhang X, Yacoub E, Hu X. New strategy for reconstructing partial-Fourier imaging data in functional MRI. *Magn Reson Med* 2001;46:1045-8.
 25. Lindholm TL, Botes L, Engman EL, et al. Parallel imaging: is GRAPPA a useful acquisition tool for MR imaging intended for volumetric brain analysis? *BMC Med Imaging* 2009;9:15.
 26. Jiang Q, Zhang ZG, Chopp M. MRI evaluation of white matter recovery after brain injury. *Stroke* 2010;41:S112-3.
 27. Wang C, Stebbins GT, Nyenhuis DL, et al. Longitudinal changes in white matter following ischemic stroke: a three-year follow-up study. *Neurobiol Aging* 2006;27:1827-33.
 28. Liu Y, D'Arceuil HE, Westmoreland S, et al. Serial diffusion tensor MRI after transient and permanent cerebral ischemia in nonhuman primates. *Stroke* 2007;38:138-45.
 29. Sotak CH. The role of diffusion tensor imaging in the evaluation of ischemic brain injury - a review. *NMR Biomed* 2002;15:561-9.
 30. Dijkhuizen RM, van der Marel K, Otte WM, et al. Functional MRI and diffusion tensor imaging of brain reorganization after experimental stroke. *Transl Stroke Res* 2012;3:36-43.
 31. Hjort N, Christensen S, Solling C, et al. Ischemic injury detected by diffusion imaging 11 minutes after stroke. *Ann Neurol* 2005;58:462-5.
 32. Engelter ST, Wetzel SG, Bonati LH, et al. The clinical significance of diffusion-weighted MR imaging in stroke and TIA patients. *Swiss Med Wkly* 2008;138:729-40.
 33. Mukherjee P, Bahn MM, McKinstry RC, et al. Differences between gray matter and white matter water diffusion in stroke: diffusion-tensor MR imaging in 12 patients. *Radiology* 2000;215:211-20.
 34. D'Arceuil HE, de Crespigny AJ. Imaging Stroke Evolution after Middle Cerebral Artery Occlusion in Non-human Primates. *Open Neuroimag J* 2011;5:216-24.
 35. Siemonsen S, Lobel U, Sedlacik J, et al. Elevated T2-values in MRI of stroke patients shortly after symptom onset do not predict irreversible tissue infarction. *Brain* 2012;135:1981-9.
 36. Jiang Q, Ewing JR, Zhang ZG, et al. Magnetization transfer MRI: application to treatment of middle cerebral artery occlusion in rat. *J Magn Reson Imaging* 2011;13:178-84.
 37. Tourdias T, Dousset V, Sibon I, et al. Magnetization transfer imaging shows tissue abnormalities in the reversible penumbra. *Stroke* 2007;38:3165-71.

38. Dani KA, An L, Henning EC, et al. Multivoxel MR spectroscopy in acute ischemic stroke: comparison to the stroke protocol MRI. *Stroke* 2012;43:2962-7.
39. Nicoli F, Lefur Y, Denis B, et al. Metabolic counterpart of decreased apparent diffusion coefficient during hyperacute ischemic stroke: a brain proton magnetic resonance spectroscopic imaging study. *Stroke* 2003;34:e82-7.
40. Demougeot C, Marie C, Giroud M, et al. N-acetylaspartate: a literature review of animal research on brain ischaemia. *J Neurochem* 2004;90:776-83.
41. Roitberg B, Khan N, Tuccar E, et al. Chronic ischemic stroke model in cynomolgus monkeys: behavioral, neuroimaging and anatomical study. *Neurol Res* 2003;25:68-78.
42. Ford CC, Griffey RH, Matwiyoff NA, et al. Multivoxel 1H-MRS of stroke. *Neurology* 1992;42:1408-12.
43. Monsein LH, Mathews VP, Barker PB, et al. Irreversible regional cerebral ischemia: serial MR imaging and proton MR spectroscopy in a nonhuman primate model. *AJNR Am J Neuroradiol* 1993;14:963-70.
44. Alf MF, Lei H, Berthet C, et al. High-resolution spatial mapping of changes in the neurochemical profile after focal ischemia in mice. *NMR Biomed* 2012;25:247-54.
45. D'Arceuil HE, Duggan M, He J, et al. Middle cerebral artery occlusion in *Macaca fascicularis*: acute and chronic stroke evolution. *J Med Primatol* 2006;35:78-86.
46. Sun PZ, Zhou J, Huang J, et al. Simplified quantitative description of amide proton transfer (APT) imaging during acute ischemia. *Magn Reson Med* 2007;57:405-10.
47. Jokivarsi KT, Hiltunen Y, Grohn H, et al. Estimation of the onset time of cerebral ischemia using T1rho and T2 MRI in rats. *Stroke* 2010;41:2335-40.
48. Gröhn OHJ, Kettunen MI, Mäkelä HI, et al. Early detection of irreversible cerebral ischemia in the rat using dispersion of the magnetic resonance imaging relaxation time, T1rho. *J Cereb Blood Flow Metab* 2000;20:1457-66.
49. Liu HS, Chung HW, Chou MC, et al. Effects of microvascular permeability changes on contrast-enhanced T1 and pharmacokinetic MR imagings after ischemia. *Stroke* 2013;44:1872-7.
50. Wu WC, Fernandez-Seara M, Detre JA, et al. A theoretical and experimental investigation of the tagging efficiency of pseudocontinuous arterial spin labeling. *Magn Reson Med* 2007;58:1020-27.
51. Li CX, Patel S, Wang DJ, et al. Effect of high dose isoflurane on cerebral blood flow in macaque monkeys. *Magn Reson Imaging* 2014. [Epub ahead of print]. Available online: [http://www.mrijournal.com/article/S0730-725X\(14\)00144-1/abstract](http://www.mrijournal.com/article/S0730-725X(14)00144-1/abstract)
52. MacIntosh BJ, Pattinson KT, Gallichan D, et al. Measuring the effects of remifentanyl on cerebral blood flow and arterial arrival time using 3D GRASE MRI with pulsed arterial spin labelling. *J Cereb Blood Flow Metab* 2008;28:1514-22.
53. Zhang X, Nagaoka T, Auerbach EJ, et al. Quantitative basal CBF and CBF fMRI of rhesus monkeys using three-coil continuous arterial spin labeling. *Neuroimage* 2007;34:1074-83.

Cite this article as: Zhang X, Tong F, Li CX, Yan Y, Nair G, Nagaoka T, Tanaka Y, Zola S, Howell L. A fast multiparameter MRI approach for acute stroke assessment on a 3T clinical scanner: preliminary results in a non-human primate model with transient ischemic occlusion. *Quant Imaging Med Surg* 2014;4(2):112-122. doi: 10.3978/j.issn.2223-4292.2014.04.06